MONITORING MICROSTRUCTURAL EVOLUTION AND CRACK FORMATION IN A SOLID PROPELLANT UNDER INCREMENTAL STRAIN CONDITION-USING DIGITAL RADIOGRAPHY X-RAY TECHNIQUES

C.T. Liu
Air Force Research Laboratory (AFMC)
10 East Saturn Boulevard
Edwards AFB, CA 93524-7680

Lee M. Klynn & Jay D. Thompson
Lockheed Martin
Advanced Technology Center
3251 Hanover Street
Palo Alto, CA 91356

ABSTRACT

In this study, the change of microstructure and the formation of cracks in a solid propellant under an incremental strain loading condition were investigated using digital radiography x-ray techniques. Experimental findings revealed that the degree of inhomogeneity of the material's microstructure and the number of non-propagating cracks increased as the applied strain was increased. Also, the strain distribution was highly non-uniform when the applied strain was high.

INTRODUCTION

It is known that throughout the loading history, the progressive development and interaction of various damage modes change the state of the material and the response of the structures. In addition to the micro-damage, large cracks can also develop in the material either during the manufacturing processes or by service loads. Therefore, to effectively use the material in structural applications one needs to understand the damage initiation and evolution processes, the effects of damage and crack development on the material's response, and the remaining strength and life of the structures.

In past years, a considerable amount of effort was spent in obtaining a fundamental understanding of damage initiation and evolution processes[1-3]. Much of what we know about the damage process under different loading conditions has been obtained using nondestructive testing techniques including ultrasonics, thermography, and x-ray radiography. Ultrasonic experimental findings revealed that damage, expressed in terms of the attenuation of the acoustic energy, increased with increasing strain rate, and the critical damage was relatively insensitive to the strain rate. Tests also revealed that the damage state correlated well with the constitutive behavior of the material. The ultrasonic technique used in this study can be used to monitor damage initiation and evolution processes in a small region of the material. In order to determine the damage field in a large area, acoustic-imaging technique was used. By using the acoustic imaging technique, the damage characteristics near the crack tip were determined. The acoustic imaging data showed that, due to the viscoelastic nature of the materials, load history and time had a significant effect on the damage characteristics in the materials

In this study, Lockheed Martin Advanced Technology Center's High-Resolution Digital X-Ray System was used to monitor the microstrucural change and the formation of cracks in a solid propellant under incremental strain loading condition.

Report Documentation Page

Form Approved
OMB No. 0704-0188

1. REPORT DATE	2. REPORT TYPE	3. DATES COVERED
02 FEB 2004		**-**

4. TITLE AND SUBTITLE	5a. CONTRACT NUMBER
Monitoring Microstructural Evolution and Crack Formation in a Solid Propellant under Incremental Strain Condition-Using Digital Radiography X-ray Techniques	5b. GRANT NUMBER
	5c. PROGRAM ELEMENT NUMBER

6. AUTHOR(S)	5d. PROJECT NUMBER
C Lui; Lee Klynn; Jay Thompson	**2302**
	5e. TASK NUMBER **0378**
	5f. WORK UNIT NUMBER **23020378**

7. PERFORMING ORGANIZATION NAME(S) AND ADDRESS(ES)	8. PERFORMING ORGANIZATION REPORT NUMBER
Air Force Research Laboratory (AFMC),AFRL/PRS,5 Pollux Drive,Edwards AFB,CA,93524-7048	

9. SPONSORING/MONITORING AGENCY NAME(S) AND ADDRESS(ES)	10. SPONSOR/MONITOR'S ACRONYM(S)
	11. SPONSOR/MONITOR'S REPORT NUMBER(S)

12. DISTRIBUTION/AVAILABILITY STATEMENT
Approved for public release; distribution unlimited

13. SUPPLEMENTARY NOTES

14. ABSTRACT
In this study, the change of microstructure and the formation of cracks in a solid propellant under an incremental strain loading condition were investigated using digital radiography x-ray techniques. Experimental findings revealed that the degree of inhomogeneity of the material's microstructure and the number of non-propagating cracks increased as the applied strain was increased. Also, the strain distribution was highly non-uniform when the applied strain was high.

15. SUBJECT TERMS

16. SECURITY CLASSIFICATION OF:			17. LIMITATION OF ABSTRACT	18. NUMBER OF PAGES	19a. NAME OF RESPONSIBLE PERSON
a. REPORT	b. ABSTRACT	c. THIS PAGE			
unclassified	**unclassified**	**unclassified**		**6**	

THE EXPERIMENTS

The microstructure change and the crack formation in a solid propellant subjected to an incremental strain loading condition were investigated using digital x-ray techniques. The propellant specimen geometries are shown in Figure 1. The specimens were bonded to aluminum tabs that attached to the stretching apparatus.

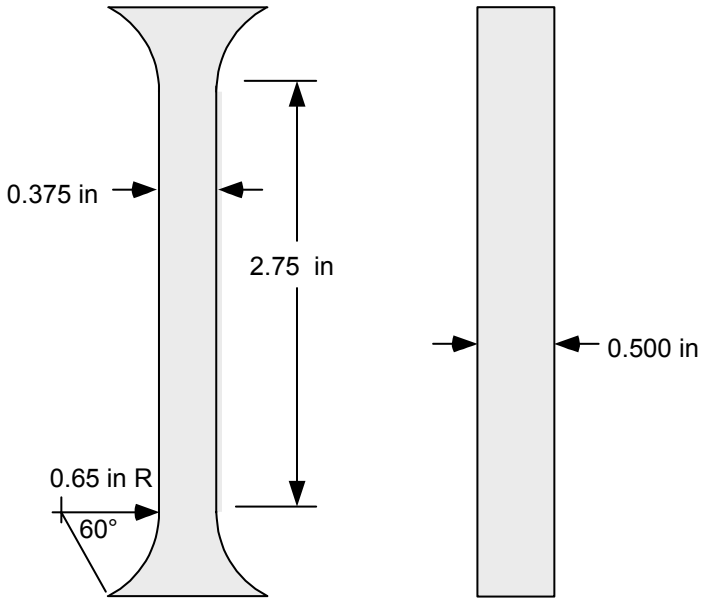

Figure 1. Specimen Dimensions

During the tests, Lockheed Martin Advanced Technology Center's High-Resolution Digital Radiography (HRDR) system was used to investigate the characteristics of the damage initiation and evolution processes. The HRDR setup for x-raying the propellant specimens is shown in Figure 2. The specimen was placed between the x-ray radiation source and the x-ray camera,with a source-to-specimen distance of 42.5 inches and a source-to-scintillator distance of 44 inches. X-ray intensity is attenuated by the propellant as described by the equation $I_x/I_i = e^{(-\mu x)}$, where I_x is the x-ray intensity passing through the propellant, I_i is the initial x-ray intensity entering the propellant, e is the natural exponential, μ is the linear x-ray attenuation coefficient, and x is the path length of the x-rays in the propellant specimen. Since propellant is a composite material, μ_x is actually the sum of all the μ_x's for the constituent materials, including air for voids and cracks. X-rays not absorbed or scattered by the propellant specimen are absorbed by the x-ray scintillator screen, which converts the x-rays into a visible light image. This image is viewed by a low-light-level CCD camera through a mirror placed at 45^o to the x-ray beam. The CCD camera converts the light image into an electrical signal that is digitized, stored, and displayed on a monitor. The x-ray images are digitized to 1024 x 1024 pixels over a 4 x 4 inch field-of-view, with 12 bits or 4096 linear intensity levels. A detailed description of the HRDR system can be found in Reference 4. When conducting the x-ray test, the 160kV x-ray source was set to 75 kV, 0.5 mA, with a 0.4 mm focal spot, without filters, and a 25-second exposure time. The combination of pixel size, geometric unsharpness, and electron range produced an effective system resolution of 0.004 inch (100 μm) in the propellant. The recorded x-ray data were processed to create a visual indication of the energy absorbed in the material. A region of high absorption (i.e., a low damage area) was shown as a dark area, whereas a region of low absorption produced a light or white area, with

4094 shades of gray in between. This is often called a positive image, unlike x-ray film which produces negative images.

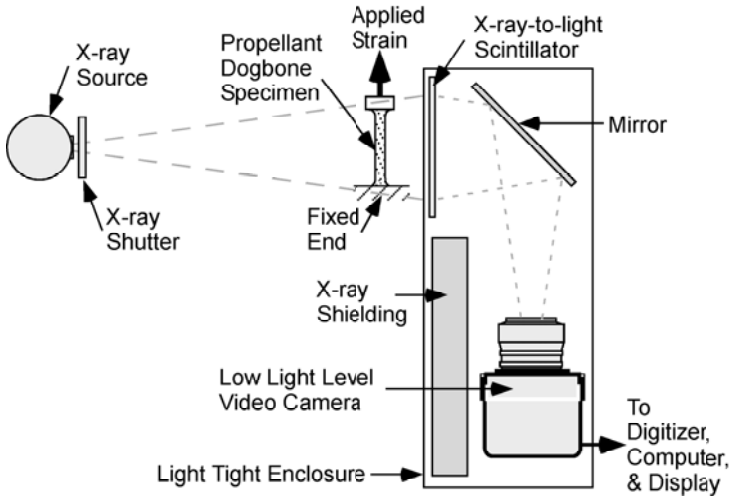

Figure 2. Testing Set-Up

RESULTS AND DISCUSSION

A highly filled polymeric material which contains a large number of fine particles, on a microscopic scale, can be considered nonhomogeneous. When this material is stretched, the different sizes and distribution of the filler particles, the different crosslinking density of the polymer chains, and the variation of the bond strength between the particles and the binder can produce highly nonhomogeneous local stress and strength fields. Because of the particle's high rigidity relative to the binder, the local stress is significantly higher than the applied stress, especially when the particles are close to each other. Since local stresses and strengths vary in a random fashion, the failure site in the material also varies randomly and does not necessarily coincide with the maximum stress location. In other words, the location and degree of damage will also vary randomly in the material. The damage may appear in the form of micro-cracks and micro-voids in the binder, or in the form of particle/binder separation known as dewetting. When the particle is dewetted, the local stresses are redistributed. With time, additional particle/binder separations and vacuole formation takes place. This time-dependent process of dewetting nucleation, or damage nucleation, is due to the time-dependent processes of stress redistribution and particle/binder separation. Depending on the formation of the material and the testing condition, damage growth may take place as material tearing or by successive nucleation and coalescence of the micro-voids. These damage initiation and evolution processes are time-dependent, and are the main factor responsible for the time-sensitivity of the strength degradation as well as the fracture behavior of the material.

The above paragraph discussed the damage mechanisms in the particle-filled polymeric material. In order to determine the change of microstructure, damage initiation and evolution, and crack formation, digital x-ray test data were analyzed. The results of the analyses are discussed in the following paragraphs.

Figure 3 shows the x-ray images at different applied strain levels. Prior to stretching the specimen, the grey level of the specimen was relatively uniform, indicating that the material's microstructure was relatively uniform. As the applied strain level was increased, the grey level varied along the length of the specimen. The non-uniform distribution of the grey level was due to the change of the microstructure of the material. The dark region was due to the high absorption of the x-ray. In other words, the densities in the dark regions were high, which implied that the

materials in the dark regions were strong. On the other hand, the light regions implied that the materials in the light regions were weak. It is interesting and important to point out that, at a critical applied strain level, a crack was formed in the weak region, and it didn't propagate. As the applied strain level was increased, the number of the non-propagating cracks increased. Finally, at 18% applied strain level, two non-propagating cracks near the center of the specimen coalesced, resulting in a long crack, which propagated and led to the fracture of the specimen. This kind of micro-structure change and crack formation process is typical for the three specimens tested.

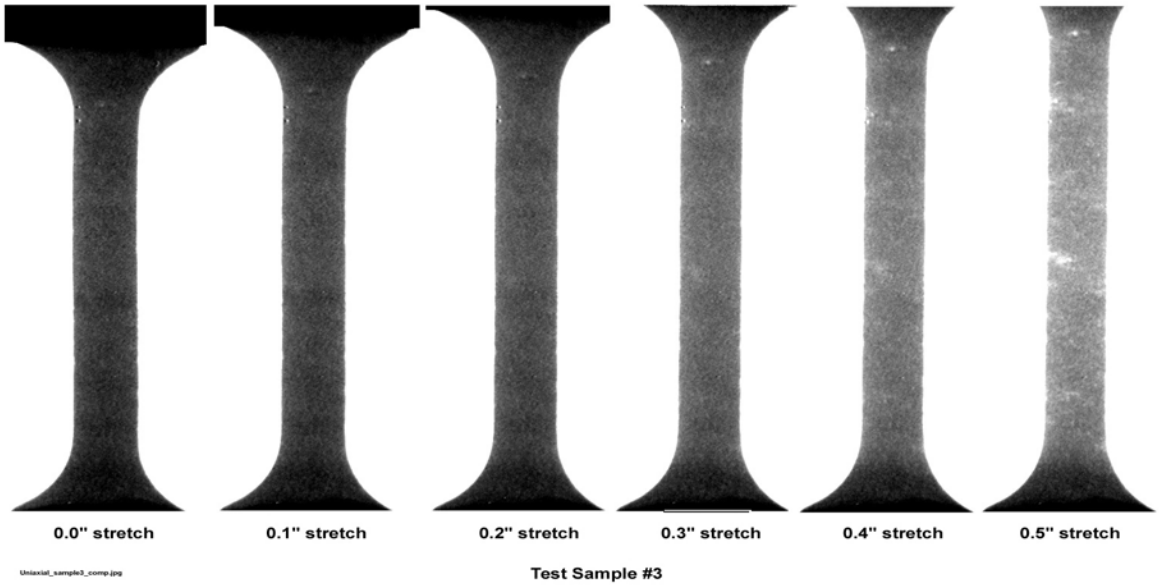

Figure 3. X-Ray Images of Sample 3 at Different Amounts of Stretch

Figure 4 is a graph of the strains in different regions of the specimens as a function of the applied strain. Five locations on the propellant specimen are labeled with markers A through E that are visible in the digital x-ray images. The position of each label was measured digitally for each stretch. The length of each section was calculated by subtracting the lower end position from the upper end position for that applied strain. The strain for each section was calculated by dividing the current incremental length by its initial length (strain = 0). From Figure 4, it is seen that the strain distribution is highly non-uniform, especially when the applied strain is high. For a given applied strain, the strain in section E-A is close to the average strain calculated by the standard method (i.e., dividing the incremental length by the effective gage length of 2.75 in). The strains in section D-C, where the two non-propagating cracks coalesce, are significantly higher than those in other sections. At 18% applied strain, which is immediately prior to specimen fracture, the strain in section D-C is 62%, whereas the strain in section E-A is 18.2%. In other words, the local failure strain is about 3.4 times higher than the global failure strain calculated by the standard method. This implies that if the failure criterion is based on the global failure strain, a safety factor of 3.4 is included in the evaluation of the structural integrity of the solid propellant grain. Referring back to Fig. 4, it is seen that the strain in section B-A starts decreasing when the applied strain reaches 7.2%, whereas the strains in other sections continue to increase. This kind of phenomenon can be explained by reviewing the x-ray data. The results of data analysis show that, by comparing the transmitted x-ray intensities I_x in sections C-B, D-C, and E-D, the I_x in section B-A is lower than those in other sections. This implies that the density in section B-A is higher than those in other sections, which in turn, implies that the material in section B-A is stronger than the materials in other sections. Under a constant applied strain condition, the

increased strains in sections C-B, D-C, and E-D will cause the strain in section B-A to decrease; the larger strains in sections C-B, D-C, and E-D produce more reduction in strain in section B-A.

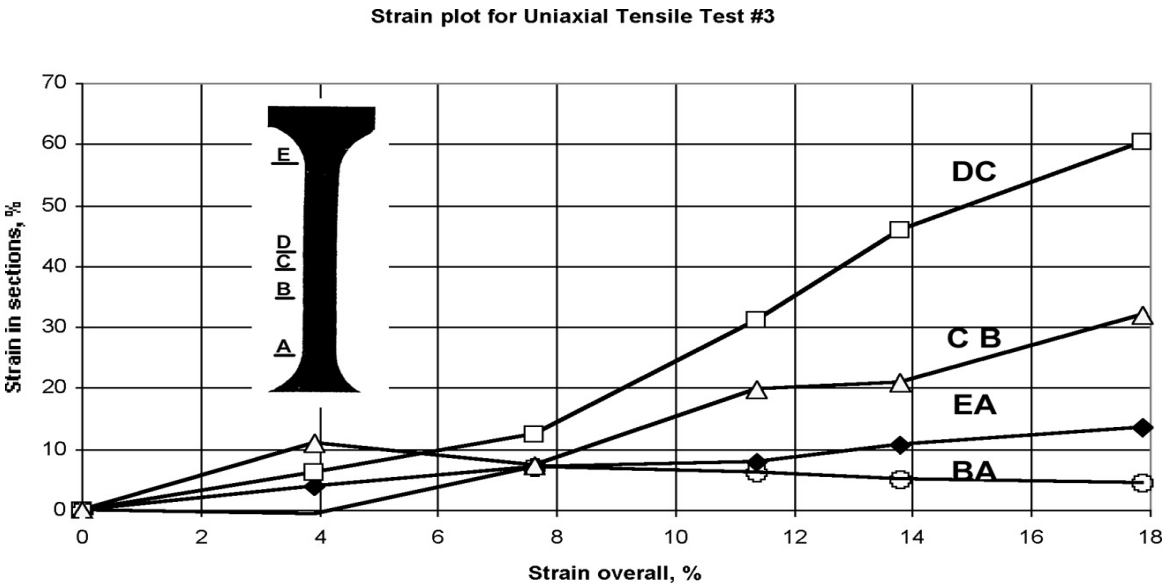

Figure 4. Section Strain as a Function of Applied Strain

Figure 5 shows difference x-ray images that indicate the change between stretches from 0 to 0.1, 0.1 to 0.2, 0.2 to 0.3, 0.3 to 0.4 and 0.4 to 0.5 inches of stretch. Each picture element (pixel) was digitally calculated by subtracting the intensity of the lower stretch from the higher stretch value. A constant value of gray was added to each pixel to avoid negative intensities. The specimens were anchored at the bottom, and the stretch was applied to the top; consequently, every location on the specimen was moving toward the top with increasing stretch. Due to the low absorption of x-ray, an inclusion will show as a dark spot on the x-ray image. On the difference image, the inclusion produces a white spot at the original location of the inclusion and a dark spot at the new location of the inclusion. Similarly, a void or a crack produces a dark spot at the original location of the void and a white spot at the new location of the void on the difference image. Changes developing in between the pair of difference images, such as new cracks or voids, are greatly emphasized. The texture shown in Figure 5 indicates relatively little disturbance in the first three difference images, and noticeable texture changes show in the last two difference images. It is interesting to point out that the white area in the last difference image, located at the middle of the left side edge of the specimen, is a crack. An indication where the crack will form can be seen in the 0.4-0.3 and perhaps in the 0.3-0.2 differences images. One can imagine it is trackable even earlier, but the x-ray image noise precludes making judgments.

CONCLUSIONS

The change of microstructure and the formation of crack in a solid propellant subjected to an incremental strain loading condition were investigated using digital x-ray techniques. Experimental findings revealed that the degree of inhomogeneity of the material's microstructure and the number of non-propagating cracks increased as the applied strain was increased. Also, the strain distribution was highly nonuniform when the applied strain was high. It also revealed that the real-time x-ray technique is a promising method to monitor microstructure changes and crack formation in solid propellants.

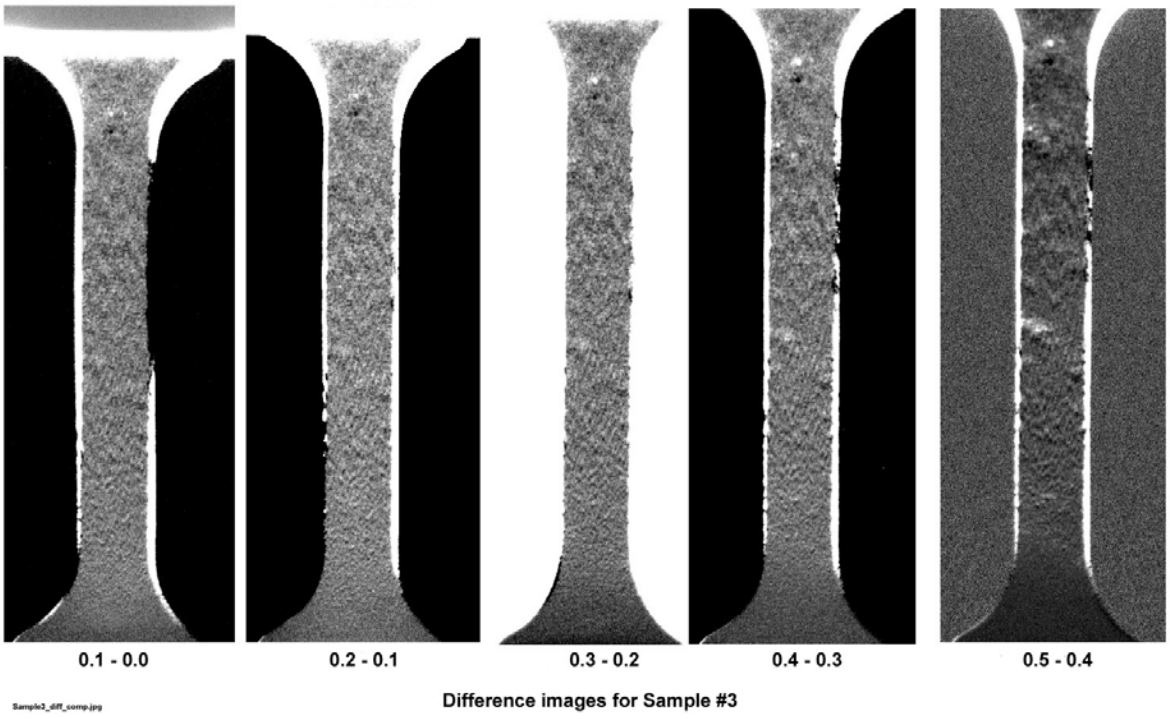

Figure 5. Digital Difference X-Ray Images of the Change from One Stretch to the Next

REFERENCES

1. Liu, C. T., "Evaluation of Damage Fields near Crack Tip in a Composite Solid Propellant," ***Journal of Spacecracfts and Rockets***, Vol. 28, No. 1, pp. 64-70, 1991.
2. Liu, C. T., "Acoustic Evaluation of Damage Characteristics in a Composite Solid Propellant", ***Journal of Spacecracfts and Rockets***, Vol. 29, No. 5, pp. 709-712, 1992.
3. Tang, B., Liu, C.T. and Henneke, E.G., "Acoustic-Ultrasonic Technique Applied to the Assessment of Damage in a Particulate Composite," ***Journal of Spacecraft and Rockets***, Vol. 32, No. 5, 1995.
4. Bueno, Cliff and Barker, Marion D., "High-Resolution Digital Radiography and Three-Dimensional Computed Tomography," ***Proceedings SPIE***, Vol. 2009, X-ray Detector Physics and Applications II, pp. 179-191, July 13-14, 1993.